

# INVESTIGATING X-RAY DETECTOR SYSTEMS USING MONTE CARLO TECHNIQUES

L. Eley<sup>1,2\*</sup>, D. Aflyatunova<sup>1</sup>, A. Hill<sup>1</sup>, C. Welsch<sup>1,2</sup>, P. Betteridge<sup>3</sup>, J. Cameron<sup>3</sup>, M. Contino<sup>3</sup>, A. Mavalankar<sup>3</sup>, S. Wells<sup>3</sup>

<sup>1</sup> Department of Physics, University of Liverpool, United Kingdom

<sup>2</sup> Cockcroft Institute, Warrington, United Kingdom

<sup>3</sup> Adaptix Ltd, Begbroke Science Park, Oxford, United Kingdom

## Abstract

Digital tomosynthesis (DT) is a 3D mode of x-ray imaging. Adaptix Ltd have developed a novel mobile DT device enabled by implementing an array of x-ray emission points with a flat-panel detector. This device sees application in human and animal scanning, as well as in non-destructive material evaluation.

DT is not as clinically popular as computed tomography (CT) or radiography, and flat-panel source DT even less so, thus creating scope to investigate the optimal flat-panel detector technology for this modality. Geant4, a Monte Carlo particle transport code, has been used to simulate the Adaptix Ltd system to do this. Parameters such as the material composition of the detectors and the exact detection method, such as the inclusion vs exclusion of a scintillation layer, is tested in this simulation environment. This work presents the method for building a simulation environment capable of investigating the optimal flat-panel detector design for this x-ray imaging technique based on Geant4 simulation results.

## INTRODUCTION

Digital tomosynthesis (DT) creates a 3D stack of image planes through an object. By varying the position of an x-ray source, multiple projections of an object can be reconstructed into a 3D image. While this method results in significantly lower patient dosage than other 3D modalities, the lack of mobility and high power requirements of this method render it relatively unpopular clinically [1]. Adaptix Ltd [2] have revised this imaging method so that instead of rotating a large x-ray tube over an arc, a stationary emitter array fires from multiple projections to allow the construction of a 3D image. This means that a low-dose, 3D x-ray image can be taken in a way that is practical for everyday medical use. Commercial devices exist currently for orthopaedic and veterinary applications, while research with the University of Liverpool is ongoing into upscaling this technology for chest scanning capabilities [3].

When comparing this modality to computed tomography, a very common competing 3D modality, the magnitude of these advantages are clear. This is highlighted especially in the mobility of the device which reduces the need for patient transport to the scanner, hence reducing hospital costs and allowing more patients to be assessed within a given

timeframe: a feature that has the potential to revolutionise modern healthcare practices [4].

For any x-ray system, the detector is a key component of the hardware. There is a large level of overlap between the detectors used for x-ray detection in synchrotron and medical contexts [5]. The considerations of the exact geometries required for a given application are very similar, including the exact detection mechanism which depends on the energy of the incident x-rays, the required pixel size for the desired image resolution and the method of electronic readout for the targeted timeframe. In both environments, these factors influence choices such as between hybrid and monolithic electronics, or photon-integrating and photon-counting set-ups.

The Adaptix Ltd device detects incident x-rays with a flat-panel digital detector. The principal advantage of these detectors over classical film screen devices is that they provide discretised information on the spatial and energy distributions of detected photons, compared to analogue data collected by film screens. Additionally, flat-panel detectors are able to create immediately readable images and have significantly better dynamic ranges than analogue screen-film outputs that require development [6]. For these reasons, flat-panel detectors are chosen as the focus of this study.

Flat-panel detectors can be classified as either direct or indirect detectors [7]. Direct flat-panel detectors measure incident x-ray photon flux, whereas indirect detectors contain a scintillating layer that converts the x-rays into optical photons to be read out electronically by devices such as CCDs. There are a large number of options for scintillating materials and the general construction of indirect and direct detectors depending on the desired properties for specific applications. Therefore, it is important that the detector chosen for a given application has properties useful in the relevant context. Some key examples of these properties include the chemical structure, rise and decay times and photon yield of the scintillator as well as the readout speed of the electronics and ability of surrounding material to limit photon signal loss.

## BUILDING THE SIMULATION

Geant4, a Monte Carlo particle transport code [8], was used to simulate the detector. In such simulations, there are a number of considerations that must be made so that the virtual environment is analogous to what would be found in reality.

\* lauryn.eley@liverpool.ac.uk

A primary example of this is the exact physics cross-sections employed by Geant4. In Geant4, the physics cross-sections are the statistical databases from which the interaction of particles with objects in the simulation environment is determined. The simulation package offers a number of electromagnetic interaction database options, including Penelope and Livermore databases. These databases are drawn from different experimental sources, and hence cause different simulated particle behaviour. It is therefore key to validate that the physics cross-sections used are realistic for the desired purpose [9]. Figure 1 shows how the x-ray spectrum created by a 90 keV electron beam incident on a tungsten target is affected by the electromagnetic settings used. While there are slight differences between the exact height of the characteristic emission and bremsstrahlung peaks for all lists tested, they are within statistical error of each other at all points and hence the Livermore list was chosen as it had the fastest run time.

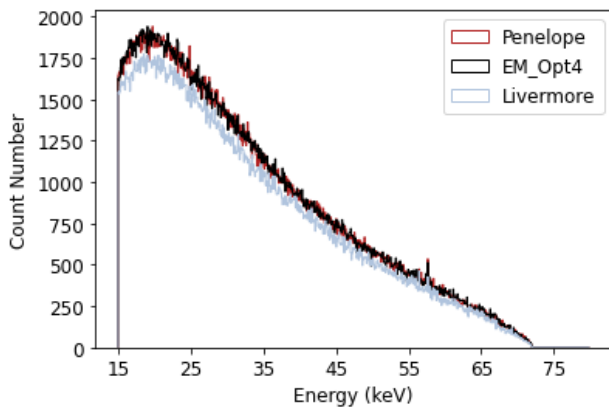


Figure 1: A comparison of the bremsstrahlung peak created by the different electromagnetic options (Livermore, Penelope, and Electromagnetic Option 4 (EMOpt4)) within Geant4.

Another consideration for the simulation environment are the range cuts chosen. The range cuts refer to the distance a simulated particle must travel for it to be created by the simulation, implemented as a way to manage CPU. Hence, the trade-off between accuracy of results and CPU time must be considered when determining what range cut is appropriate for the simulation. For this simulation, 5  $\mu\text{m}$  was found to be the optimal compromise for this metric. Table 1 displays this alongside the key simulation parameters which are a primary step in building the simulation environment.

Adaptix Ltd's DT device utilises an indirect flat-panel detector. As already briefly alluded to, for indirect detectors, the scintillator is an element of key interest for this study. The detector in question contains a Caesium Iodide (CsI) crystal scintillator for optical photon conversion. Unlike for electromagnetic physics, Geant4 handles optical physics with numerical methods rather than physics cross-sections. This means that when the scintillator is the single layer present in the simulation environment, one would expect a linear

Table 1: Physics Settings for the Simulation

Setting	Value
Base Physics List	<i>FTFP BERT</i>
EM Physics List	<i>Livermore</i>
Seeding	<i>CHLEP</i>
Range Cut	5 $\mu\text{m}$
Number of Events	1e4

increase in photon yield with scintillator thickness due to the presence of more atoms for photon production. This becomes more complex as extra layers are added in to the simulation, such as the detector casing, x-ray shielding and scintillator substrate which have unique reflectivities, refractive indices and absorption lengths for optical photons. Hence, a key element of creating this simulation is accessing this data reliably through literature; especially as this is the numerical data Geant4 relies on for handling this optical output. The number of chosen parameters is too large to include in the body of this discussion but this step is highlighted due to its high importance for creating the environment.

An interesting consideration in translating this detector technology into the Geant4 simulation environment is how best to handle the electronic component. Geant4, as a particle transport code, is not designed with the capability to directly simulate the behaviour of electronic components like CCDs or TFTs. This work sets up an analogous method which makes use of Geant4's 2D histogram sensitive detector handling. This creates a pixel-wise approach to photon counting as the detecting area is split up into individual bins of customisable size; allowing readout of photons per bin in the same way a TFT counts photons per pixel. There is an inevitable trade-off between bin size and simulation runtime: the runtime exponentially increases as the grid size increases, which illustrates the importance of considering CPU when changing the grid size.

These settings together therefore create an environment which the characteristics of the detector can be altered to allow observation of the effect on image quality and patient dosage: the key trade-off for any x-ray scanning device.

## RESULTS

The main focus of this work until now has been in building a reliable simulation framework to perform investigations in, and some preliminary results have been collected on the effect of the scintillator material on the photons produced. Figure 2 shows this for a sodium iodide (NaI), caesium iodide (CsI) and bismuth germanate (BGO) scintillator.

Figure 2 shows the expected linearity for the increasing scintillator thickness. There are additional layers present in the geometry alongside the scintillator, but as they are behaving uniformly at each scintillator thickness, this linearity is not affected. The gradient of the line corresponds to the photon yield of the scintillator where CsI has the highest yield per unit energy, at  $(5.4 \times 10^4)$  photons per MeV),

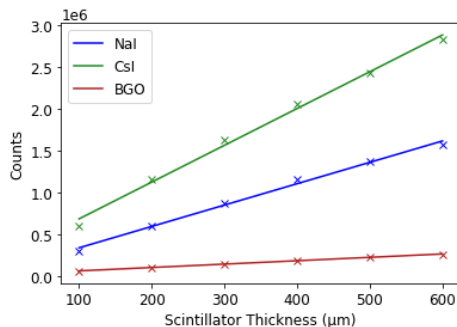


Figure 2: Photon yield with thickness from 3 different scintillators: Caesium Iodide (CsI), Sodium Iodide (NaI) and Bismuth Germanate (BGO). In this figure, the crosses show the measured data with solid regression lines plotted.

compared to BGO, with  $(8.5 \times 10^3$  photons per MeV). The average energy of the photons produced by each scintillator doesn't vary greatly nor vary with thickness, with the mean energies being  $(2.5785 \pm 0.0003)$  eV,  $(2.4853 \pm 0.0001)$  eV and  $(2.4302 \pm 0.0002)$  eV for BGO, NaI and CsI respectively. The differences in these mean photon energies arise as a result of the unique optical emission spectra associated with each scintillating material.

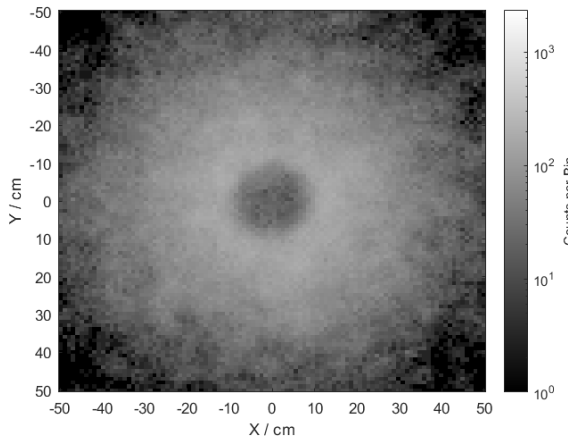


Figure 3: The shadow of a cylindrical aluminium phantom as created by a BGO scintillator detector.

Figure 3 demonstrates an image output from the created simulation environment. In this image, a cylindrical aluminium phantom centred around the detector centre is present. A BGO scintillator converts the incident x-rays to optical photons, which are detected to create the image shown. As previously outlined, each image is split into bins to imitate electronic pixels which count the number of incident optical photons per bin to create the image seen.

Figure 4 is included for comparison to Fig. 3. The photon yield per unit energy is significantly higher from the CsI scintillator than the BGO scintillator as evidenced from the significantly higher count number. This results in a sharper shadow of the imaged object as well as higher contrast be-

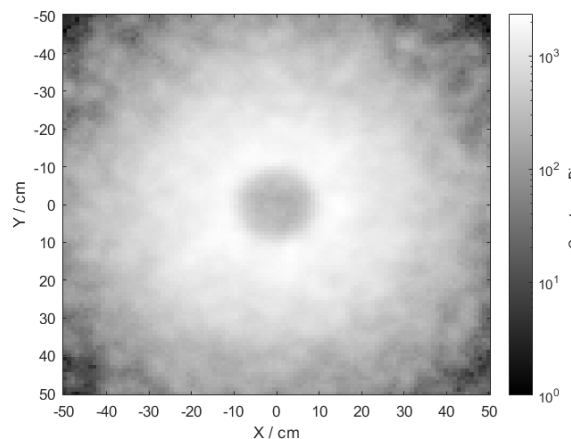


Figure 4: The shadow of a cylindrical aluminium phantom as created by a CsI scintillator detector.

tween the areas that are exposed directly to the beam and those resulting from photon scatter.

## CONCLUSION AND FUTURE WORK

This paper discusses the key considerations required in building an accurate simulation environment to perform investigations into the optimal detector for DT applications. The fundamental solutions that must be found before data collecting have been outlined, and some preliminary results have been extracted. While presented here in an x-ray medical imaging context, the approaches taken within this paper are applicable to detector investigations necessary in multiple scientific areas, such as within the detection of x-rays produced by synchrotrons for XFEL and phase-space imaging measurements.

With the reliable basis presented in this paper, a wider variety of investigations can be performed to observe the optimal construction for Adaptix Ltd's DT method. By varying the location of the x-ray source to create multiple projections for 3D image reconstruction, this study in full will allow the identification of the key detector properties for this method. This will allow better characterisation of detector quality for this application compared to other x-ray imaging modalities. Successful benchmarking of this data with images taken on the existing DT device will allow the output from the simulation to be more alike that outputted experimentally. This means real objects imaged by the device can be simulated, allowing closer comparison than previously achievable.

## ACKNOWLEDGEMENTS

This work was jointly supported by Adaptix Ltd and the Science and Technology Facilities Council (STFC) under grant agreement ST/W006766/1.

## REFERENCES

[1] J. T. Dobbins and D. J. Godfrey, "Digital x-ray tomosynthesis: Current state of the art and clinical potential", *Physics in*

*Medicine & Biology*, vol. 48, R65, 19 2003. 10.1088/0031-9155/48/19/R01

[2] *Adaptix Ltd.* <https://adaptix.com/>

[3] T. Primidis, “Design and Optimisation of Ultra-Compact, High-Resolution, 3D X-ray Imaging Systems”, Ph.D. dissertation, University of Liverpool, 2022.

[4] J. Cant, A. Snoeckx, G. Behiels, P. M. Parizel, and J. Sijbers, “Can portable tomosynthesis improve the diagnostic value of bedside chest x-ray in the intensive care unit? A proof of concept study”, *European Radiology Experimental*, 2017.

[5] T. Hatsui and H. Graafsma, “X-ray Imaging Detectors for Synchrotron and XFEL sources”, *IUCrJ*, vol. 2, no. 3, pp. 371–383, 2015.

[6] A. Del Guerra, *Ionizing Radiation Detectors for Medical Imaging*. World Scientific, 2004.

[7] Y. Izumi *et al.*, “Development of flat panel x-ray image sensors”, *Sharp Technical Journal*, 2001.

[8] S. Agostinelli *et al.*, “Geant4—a simulation toolkit”, *Nuclear Instruments and methods in physics research section A: Accelerators, Spectrometers, Detectors and Associated Equipment*, vol. 506, 2003.

[9] P. Arce, J. I. Lagares, J. D. Azcona, and P.-B. Aguilar-Redondo, “A proposal for a Geant4 physics list for radiotherapy optimized in physics performance and CPU time”, *Nuclear Instruments and Methods in Physics Research Section A: Accelerators, Spectrometers, Detectors and Associated Equipment*, vol. 964, p. 163 755, 2020.